# Continuous Higher Order Sliding Mode Control with Adaptation of Air Breathing Hypersonic Missile

Polk Yu[1] and Yuri Shtessel[2]
*University of Alabama in Huntsville, Huntsville, AL, 35899*

*and*

Christopher Edwards[3]
*University of Exeter, Exeter UK EX4 4QF, UK*

**Abstract:** Hypersonic missile control in the terminal phase is addressed using continuous higher order sliding mode (AHOSM) control with adaptation. The AHOSM self-tuning controller is proposed and studied. The double-layer adaptive algorithm is based on equivalent control concepts and ensures non-overestimation of the control gain to help mitigates control chattering. The proposed continuous AHOSM control is validated via simulations of a hypersonic missile in the terminal phase. The robustness and high accuracy output tracking in the presence of matched and unmatched external disturbances and missile model uncertainties is demonstrated.
**Key words:** Higher order sliding mode control, Adaptive control, Hypersonic missile

## I. Introduction

Controlling Hypersonic Missiles (HSM) represnts a serious challenge [1-6,14,17] for designing suitable guidance and autopilot/control (G&C) laws. The following represent the main G&C design challenges:

1. Uncertain dynamics of the HSM frame, which are difficult to predict based on ground tests.
2. The nonminimum phase behavior caused by elevator-to-lift coupling and the flexible mode dynamics.
3. The multiplicative uncertainties that mostly depend on significantly uncertain elements in aerodynamics coefficients, and their effect on the control efficiency is hard to predict.

A control-oriented model of the Hypersonic *Vehicle* with curve-fitted approximations of the aerodynamic forces and moments [2] is often used for robust controller design. Then an adaptation technique is employed for estimating the unknown *constant* coefficients used in the approximations [11]. However, in the presence of time-varying uncertain coefficients, the accuracy of the control adaptation can be compromised.

In this paper control of the Hypersonic *Missile* in the terminal phase of the flight is considered. In order to maximize the ground target penetration, the desired vertical orientation of the HSM at the impact is to be achieved [3]. Note that very few guidance and autopilot (control) laws have been designed to maximize target penetration in a target impact (terminal phase) scenario [3] while controlling the nonlinear highly uncertain HSM. Previously HOSM control

[1] Graduate student, Department of Electrical and Computer Engineering, 301 Sparkman Drive, email: pyu.hok@gmail.com
[2] Professor, Department of Electrical and Computer Engineering, 301 Sparkman Drive, Associate Fellow AIAA, Senior Member IEEE. email: shtessy@uah.edu, tel: (256)-824-6164, fax: (256) 824-6803, corresponding author
[3] Professor, College of Engineering, Mathematics and Physical Sciences, email: c.edwards@exeter.ac.uk

and observation techniques have been effectively applied for missile-interceptor integrated guidance and autopilot/control [12,13]. In this work a continuous Adaptive Higher Order Sliding Mode [9,10,15] (AHOSM) controller that comprises Continuous Finite Time Convergent Control [8] driven by a higher order sliding mode disturbance observer [15] is employed to design the HSM integrated guidance and autopilot, to track the terminal phase optimal trajectory in the presence of additive (external disturbances and the model uncertainties) and multiplicative (aerodynamic coefficient uncertainties) perturbations. Furthermore, in order to mitigate any residual control chattering caused by the high frequency switching term hidden behind the integral in the injection term of the HOSM disturbance observer, an adaptive (self-tuning) scheme is proposed. The proposed double-layer gain-adaptation algorithms is based on the concept of *equivalent control* [16] and yields a non-overestimating adaptive gain that closely follows the disturbance. Curve-fitted approximations of the aerodynamic forces and moments are not used in the proposed control design approach.

The proposed AHOSM integrated guidance and autopilot (control) law is rigorously studied for a HSM in the terminal phase and its efficacy is verified via simulations.

## I. Mathematical Model of Air-Breathing Hypersonic Missile

The mathematical model of the longitudinal dynamics of the rigid body hypersonic missile (see Figs. 1 and 2 [3]) that is propelled by an air-breathing jet engine (usually a scramjet) is considered as [1,2]

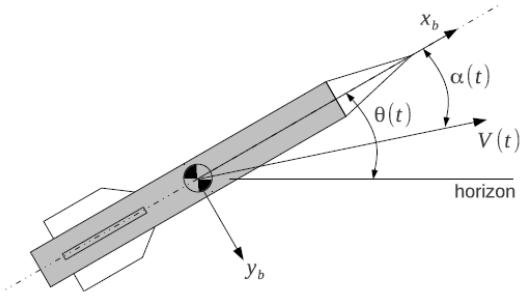


Fig. 1 HSM coordinate frames and longitudinal variables

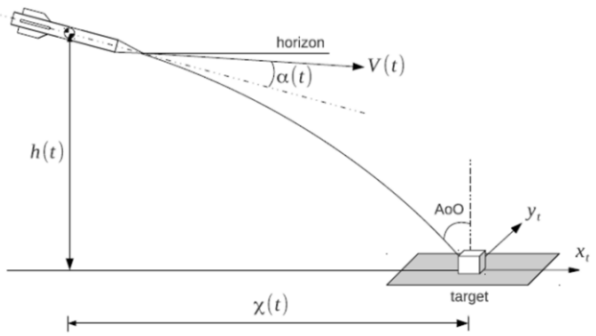


Fig. 2 HSM-target end-game scenario

$$\begin{cases} \dot{V} = \dfrac{T\cos(\alpha) - D}{m} - g\sin(\theta - \alpha) \\ \dot{h} = V\sin(\theta - \alpha) \\ \dot{\alpha} = -\dfrac{L + T\sin(\alpha)}{mV} + q + \dfrac{g}{V}\cos(\theta - \alpha) \\ \dot{\theta} = q \\ \dot{q} = \dfrac{M}{I_{yy}} \\ \dot{\chi} = V\cos(\theta - \alpha) \end{cases} \tag{1}$$

where $V(t) \in \mathbb{R}$ denotes the forward velocity; $h(t) \in \mathbb{R}$ denotes the HSM altitude; $\alpha(t) \in \mathbb{R}$ denotes the angle of attack; $\theta(t), q(t) \in \mathbb{R}$ denote the pitch angle and the pitch rate respectively; $\chi(t) \in \mathbb{R}$ denotes the downrange distance (see Fig. 2) measured with respect to the initial HSM position; $m, I_{yy} \in \mathbb{R}$ denote the mass and the moment of inertia about the HSM body *y*-axis respectively; $g \in \mathbb{R}$ is gravitional acceleration; $T, D, L \in \mathbb{R}$ denote the thrust, drag, and lift forces, respectively; $M \in \mathbb{R}$ is the pitching moment about the body *y*-axis. In the longitudinal dynamics (1) the flexible modes associated with aero-thermo-elastic effects are neglected for simplicity. The thrust $T$, drag $D$, and lift $L$ forces, as well as the pitching moment $M$ about the body *y*-axis are nonlinear uncertain functions that can be given as [2-4]

$$L = L(\alpha, \delta_e),\ D = D(\alpha, \delta_e),\ M = M(T, \alpha, \delta_e),\ T = T(\phi, \alpha) \tag{2}$$

where $\delta_e(t) \in \mathbb{R}$ denotes the elevator surface deflection, and $\phi \in \mathbb{R}$ is the dimensionless fuel-to-air ratio ($\phi \in [0, 1.5]$).

The control vector is

$$u = [\phi, \delta_e]^T \tag{3}$$

while the vector of controlled outputs is selected as

$$y = [h, \theta]^T. \tag{4}$$

Unlike in the existing literature on Hypersonic *Vehicle* control [4-6], where the control output $y = [h, V]^T$ is driven to a constant vector after a short transient when the velocity and altitude are commanded to increase from zero to the prescribed constant values, the work presented here considers control of a Hypersonic Missile (HSM) in the end-game scenario with a different vector-output (4) and time-varying commanded output trajectories (see also Fig. 2)

$$y_c(t) = [h_c(t), \theta_c(t)]^T \tag{5}$$

The goal of the considered end-game scenario is to maximize target penetration by means of generating the optimal end-game HSM trajectory (5) for system (1) and robustly following this trajectory by means of control (3) in the presence of the bounded perturbations (2).

The optimal command trajectory is obtained in [3] by minimizing the following cost functional:

$$\begin{aligned} &J = \left[x(t_f) - x_c(t_f)\right]^T \Gamma \left[x(t_f) - x_c(t_f)\right], \\ &x = [V, \alpha, q, h, \theta]^T \end{aligned} \tag{6}$$

where $\Gamma \in \mathbb{R}^{5\times5}$ is a positive definite weighting matrix, and $x_c(t_f)$ denotes the desired final value of the state $x$. The terminal conditions on the state $x$ are defined to ensure $\theta = -90^0$ and the angle of obliquity (AoO in Fig. 2) is equal to zero at impact:

$$V(t_f) = V_f\,[\,ft/s],\ \alpha(t_f) = 0[\deg],\ q(t_f) = 0[\deg/s],\ h(t_f) = 0[\,ft],\ \theta(t_f) = -90[\deg] \tag{7}$$

The solution of the trajectory optimization problem is obtained numerically [3] and the optimal output command trajectories in eq. (5), (6) are used for the robust output feedback tracking controller design.

***Remark 1.*** In this work, the lift-elevator coupling, which usually represents the main source of instability of the internal/zero dynamics, is neglected. In the case of significant coupling, canards may be added to HSM to compensate it.

## II. Relative Degree Approach: System Transformation and Problem Formulation

In order to achieve continuity of the control functions, in this work, a HOSM control law is designed in term of derivatives of the control functions (3) as

$$v = [v_1, v_2]^T = \left[\dot{\phi}, \dot{\delta}_e\right]^T \tag{8}$$

Designing the control law in terms of control derivatives serves two purposes:

- A curve-fitted approximation of the aerodynamic forces and moments is not needed in the proposed control design approach and knowledge of the aerodynamic coefficients is not required for the controller (8) design.
- It mitigates noise/chattering effects.

Next, applying the relative degree approach [3], the input-output dynamics of system (1), (4), (8) are derived as

$$\begin{bmatrix}\theta^{(3)}\\ h^{(3)}\end{bmatrix} = \begin{bmatrix}\psi_\theta(\theta,\phi,\delta_e,\alpha,q,V)\\ \psi_h(\theta,\phi,\delta_e,\alpha,q,V)\end{bmatrix} + \begin{bmatrix}g_{11} & g_{12}\\ g_{21} & g_{22}\end{bmatrix}\begin{bmatrix}v_1\\ v_2\end{bmatrix} + \begin{bmatrix}\Delta g_{11} & \Delta g_{12}\\ \Delta g_{21} & \Delta g_{22}\end{bmatrix}\begin{bmatrix}v_1\\ v_2\end{bmatrix} \tag{9}$$

where the control gain matrix $G \in \mathbb{R}^{2\times 2}$

$$G = \begin{bmatrix}\dfrac{1}{I_{yy}}\dfrac{\partial M(\phi,\alpha,\delta_e)}{\partial \phi} & \dfrac{1}{I_{yy}}\dfrac{\partial M(\phi,\alpha,\delta_e)}{\partial \delta_e}\\ \dfrac{1}{m}\dfrac{\partial T(\phi,\alpha)}{\partial \phi}\sin(\theta) & \dfrac{1}{m}\left[\dfrac{\partial L(\alpha,\delta_e)}{\partial \delta_e}\cos(\theta-\alpha) - \dfrac{\partial D(\alpha,\delta_e)}{\partial \delta_e}\sin(\theta-\alpha)\right]\end{bmatrix} \tag{10}$$

is assumed to be nonsingular and is presented as

$$G = G_0 + \Delta G = \underbrace{\begin{bmatrix}g_{11} & g_{12}\\ g_{21} & g_{22}\end{bmatrix}}_{G_0} + \underbrace{\begin{bmatrix}\Delta g_{11} & \Delta g_{12}\\ \Delta g_{21} & \Delta g_{22}\end{bmatrix}}_{\Delta G} \tag{11}$$

with $G_0$ denoting a known nonsingular nonlinear matrix and $\Delta G$ denoting an unknown norm-bounded nonlinear matrix.

The following notations are introduced:

$$\psi_\theta(\theta,\phi,\delta_e,\alpha,q,V) = \frac{1}{I_{yy}}\frac{\partial M(\phi,\alpha,\delta_e)}{\partial \alpha}\left[-\frac{L(\alpha,\delta_e)+T(\phi,\alpha)\sin(\alpha)}{mV} + q + \frac{g}{V}\cos(\theta-\alpha)\right]$$

$$\psi_h(\theta,\phi,\delta_e,\alpha,q,V) = \frac{1}{m}\left[\frac{\partial T(\phi,\alpha)}{\partial \alpha}\sin(\theta) - \frac{\partial D(\alpha,\delta_e)}{\partial \alpha}\sin(\theta-\alpha)\right]\left[-\frac{L(\alpha,\delta_e)+T(\phi,\alpha)\sin(\alpha)}{mV} + q + \frac{g}{V}\cos(\theta-\alpha)\right] -$$

$$\frac{1}{m}\left[\frac{L(\alpha,\delta_e)+T(\phi,\alpha)\sin(\alpha)}{mV} - \frac{g}{V}\cos(\theta-\alpha)\right]\left[D(\alpha,\delta_e)\cos(\theta-\alpha) + L(\alpha,\delta_e)\sin(\theta-\alpha)\right] +$$

$$\frac{1}{m}T(\phi,\alpha)q\cos(\theta) + \frac{1}{m}\frac{\partial L(\alpha,\delta_e)}{\partial \alpha}\left[-\frac{L(\alpha,\delta_e)+T(\phi,\alpha)\sin(\alpha)}{mV} + q + \frac{g}{V}\cos(\theta-\alpha)\right]\cos(\theta-\alpha)$$

Next, the problem is reduced to designing the control law (8) that drives $h(t)\to h_c(t)$ and $\theta(t)\to\theta_c(t)$ in finite time in the presence of the bounded disturbances $\psi_\theta(\theta,\phi,\delta_e,\alpha,q,V)$, $\psi_h(\theta,\phi,\delta_e,\alpha,q,V)$ and the norm-bounded matrix $\Delta G$, where $h_c(t)$ and $\theta_c(t)$ are the smooth command trajectories defined by eqs. (5) and (6).

Denoting

$$\begin{bmatrix} g_{11} & g_{12} \\ g_{21} & g_{22} \end{bmatrix}\begin{bmatrix} v_1 \\ v_2 \end{bmatrix}=\begin{bmatrix} \omega_1 \\ \omega_2 \end{bmatrix} \;\Rightarrow\; \begin{bmatrix} v_1 \\ v_2 \end{bmatrix}=\begin{bmatrix} g_{11} & g_{12} \\ g_{21} & g_{22} \end{bmatrix}^{-1}\begin{bmatrix} \omega_1 \\ \omega_2 \end{bmatrix}$$
$$\begin{bmatrix} \Delta g_{11} & \Delta g_{12} \\ \Delta g_{21} & \Delta g_{22} \end{bmatrix}\begin{bmatrix} g_{11} & g_{12} \\ g_{21} & g_{22} \end{bmatrix}^{-1}=\begin{bmatrix} d_{11} & d_{12} \\ d_{21} & d_{22} \end{bmatrix} \tag{12}$$

and substituting into eq. (10) we obtain

$$\begin{cases} \theta^{(3)}=\psi_\theta(\theta,\phi,\delta_e,\alpha,q,V)+d_{12}\omega_2+(1+d_{11})\omega_1 \\ h^{(3)}=\psi_h(\theta,\phi,\delta_e,\alpha,q,V)+d_{21}\omega_1+(1+d_{22})\omega_2 \end{cases} \tag{13}$$

The output tracking errors are defined as

$$e_\theta=\theta_c(t)-\theta(t),\;\; e_h=h_c(t)-h(t) \tag{14}$$

and the error-dynamics are derived

$$\begin{cases} e_\theta^{(3)}=\underbrace{\theta_c^{(3)}(t)-\left(\psi_\theta(\theta,\phi,\delta_e,\alpha,q,V)+d_{12}\omega_2+d_{11}\omega_1\right)}_{\Psi_\theta}-\omega_1 \\ e_h^{(3)}=\underbrace{h_c^{(3)}(t)-\left(\psi_h(\theta,\phi,\delta_e,\alpha,q,V)+d_{21}\omega_1+d_{22}\omega_2\right)}_{\Psi_h}-\omega_2 \end{cases} \tag{15}$$

The following assumptions are made:

*Assumption 1.* The derivatives of the nonlinear terms $\Psi_\theta(\theta,\phi,\delta_e,\alpha,q,V,d_{12},\omega_2)$, $\Psi_h(\theta,\phi,\delta_e,\alpha,q,V,d_{21},\omega_1)$ are norm-bounded in a reasonable flight domain, i.e.

$$\begin{aligned} &\left|\dot\Psi_\theta(\theta,\phi,\delta_e,\alpha,q,V,d_{12},\omega_2)\right|\le C_\theta, \\ &\left|\dot\Psi_h(\theta,\phi,\delta_e,\alpha,q,V,d_{21},\omega_1)\right|\le C_h,\quad C_\theta,C_h>0. \end{aligned} \tag{16}$$

*Assumption 2.* The nonlinear terms $d_{11},d_{12},d_{21},d_{22}$ are also bounded in a reasonable flight domain, i.e.

$$|d_{11}|\le\varepsilon_{11},|d_{12}|\le\varepsilon_{12},|d_{21}|\le\varepsilon_{21},|d_{22}|\le\varepsilon_{22},\;\varepsilon_{11},\varepsilon_{12},\varepsilon_{21},\varepsilon_{22}>0,\;\varepsilon_{11}+\varepsilon_{12}<1,\;\varepsilon_{21}+\varepsilon_{22}<1 \tag{17}$$

Inequalities (17) guarantee the dominance of the control functions $\omega_i, i=1,2$ in the $i^{th}$, $i=1,2$ channels over the perturbations, including cross-coupling between the channels.

Finally, the problem is reduced to designing the continuous control law $\omega=\begin{bmatrix}\omega_1 & \omega_2\end{bmatrix}^T$ that provides convergence $e_\theta,\; e_h\to 0$ in finite time for perturbed system (15)-(17).

## III. Continuous Finite Time Convergent Control Driven by the Disturbance Observer

Consider SISO input-output dynamics of the form [15]

$$\sigma^{(r)}=\varphi(t)+u, \tag{18}$$

where $u\in\mathbb{R}$, $\sigma\in\mathbb{R}$ are control and output variables, respectfully, and $\varphi(t)$ is a disturbance. The following theorem gives a control law that provides finite time convergence in the unperturbed version of system (18).

***Theorem 1* [8]** Consider the *unperturbed* system (18) with $\varphi(t)\equiv 0$. Let the $\gamma_i>0$ be such that the polynomial $s^r+\gamma_r s^{r-1}+...+\gamma_2 s+\gamma_1$ is Hurwitz, then there exists $\varepsilon\in(0,1)$ such that for every $\alpha\in(1-\varepsilon,1)$ the origin of the system (18), $\sigma=\dot\sigma=...=\sigma^{(r-1)}=0$ is a globally finite-time stable equilibrium under the feedback control

$$u=-\gamma_r\left|\sigma^{(r-1)}\right|^{\alpha_r}sign\left(\sigma^{(r-1)}\right)-\gamma_{r-1}\left|\sigma^{(r-2)}\right|^{\alpha_{r-1}}sign\left(\sigma^{(r-2)}\right)-...-\gamma_1|\sigma|^{\alpha_1}sign(\sigma) \tag{19}$$

where the coefficients $\alpha_1,\alpha_2,...,\alpha_r$ satisfy

$$\alpha_{i-1}=\frac{\alpha_i\alpha_{i+1}}{2\alpha_{i+1}-\alpha_i},\quad i=2,...r \tag{20}$$

with $\alpha_{r+1}=1,\ \alpha_r=\alpha$.

***Remark 2.*** It is worth noting that the control (19), (20) is continuous.

## A. Continuous HOSM Control Design

The theoretical result that allows designing a finite-time converging continuous control for the perturbed system (18) is formulated in the following theorem.

***Theorem 2.*** Consider the *perturbed* system (18) with smooth $\varphi(t)\neq 0$ so that $|\dot\varphi(t)|\le H$. Let $\gamma_i>0$ be such that the polynomial $s^r+\gamma_r s^{r-1}+...+\gamma_2 s+\gamma_1$ is Hurwitz, and $\varepsilon\in(0,1)$ is identified so that the *unperturbed* system (18) is finite-time convergent with the control feedback (19), (20). Then the origin of the perturbed system (18), $\sigma=\dot\sigma=...=\sigma^{(r-1)}=0$ is a globally finite-time stable equilibrium under the continuous control feedback

$$u=-\gamma_r\left|\sigma^{(r-1)}\right|^{\alpha_r}sign\left(\sigma^{(r-1)}\right)-\gamma_{r-1}\left|\sigma^{(r-2)}\right|^{\alpha_{r-1}}sign\left(\sigma^{(r-2)}\right)-...-\gamma_1|\sigma|^{\alpha_1}sign(\sigma)-\varpi \tag{21}$$

where

$$s=\sigma^{(r-1)}+z,\quad \dot z=-u-\varpi \tag{22}$$

$$\begin{aligned}&\varpi=\eta_1|s|^{1/2}sign(s)+\xi\\&\dot\xi=\eta_2 sign(s),\quad \eta_1=1.5H^{1/2},\ \eta_2=1.1H\end{aligned} \tag{23}$$

**Proof.** The $s$ – dynamics in (22) satisfy

$$\dot s=\varphi(t)-\varpi \tag{24}$$

in accordance with eq. (18). Then the super-twisting control [10]

$$\begin{aligned}&\varpi=\eta_1|s|^{1/2}sign(s)+\xi\\&\dot\xi=\eta_2 sign(s)\end{aligned} \tag{25}$$

with

$$\eta_2>H, \tag{26}$$

$$\eta_1>\sqrt{\frac{2}{\eta_2-H}}\frac{(\eta_2+H)(1+q)}{1-q} \tag{27}$$

where $|\varphi(t)|<q\Omega_m,\ 0<q<1,\ |\varpi|\le\Omega_m$ drives $s,\dot s\to 0$ in finite time $t_1$. It is also known [10, 15] that choosing $\eta_1=1.5H^{1/2},\ \eta_2=1.1H$ drives $s,\dot s\to 0$ in finite time as well.

Therefore $\varpi$ becomes equal to $\varphi(t)$ for $\forall t \geq t_1$. Hence, the control (21) starts compensating for the disturbance $\varphi(t)$ for $\forall t \geq t_1$, and the system (18) becomes unperturbed. Then, in accordance with Theorem 1 the origin $\sigma = \dot{\sigma} = ... = \sigma^{(r-1)} = 0$ is globally finite-time stable, and the theorem is proven.

***Remark 3.*** The continuous controller (21)-(23) can be claimed to be a continuous HOSM controller for the system in (18), since it drives $\sigma, \dot{\sigma}, ..., \sigma^{(r-1)} \to 0$ in finite time in the presence of the smooth disturbance $\varphi(t)$ with bounded derivative $|\dot{\varphi}(t)| \leq H$.

## B. Adaptive Continuous HOSM Control Design: Equivalent Control Approach

As argued in the previous section, the continuous HOSM in (13) contains the term $\varpi$ that represents a reconstruction of the unknown disturbance term $\varphi(t)$.The super-twisting injection term in (21) contains a component $\xi$, whose derivative is a discontinuous high frequency switching function with gain $\eta_2 > H$. In order to reduce chattering, it is desirable to make $\eta_2$ as close to $H$ as possible whilst ensuring $\eta_2 > H$. Therefore, assuming that the gain $\eta_1$ can be selected large enough so that the second equation in (27) holds, the aim is to adapt $\eta_2$ in equation (26) so that $\eta_2$ is close to $H$ whilst satisfying condition in (26). This self-tuning procedure reduces the amplitude of the high frequency part of the super-twisting term in equation (25), which mitigates chattering. In this paper an adaptive scheme built on the *equivalent control* [16] is employed.

### *B.1 Equivalent control in super-twisting control adaptation*

Consider the super-twisting structure arising from equations (24) and (25) written out in a transformed form as

$$\begin{aligned} \dot{s} &= -\eta_1 |s|^{1/2} sign(s) + \xi_2 \\ \dot{\xi}_2 &= \zeta(t) - w(t) \end{aligned} \tag{28}$$

where $\zeta(t) = \dot{\varphi}(t)$ and

$$w(t) = k(t) sign(s) \tag{29}$$

The goal is to derive an adaptive scheme for the time-varying gain $k(t)$ so that a 2SM is achieved and maintained, but which also attempts to ensure $k(t)$ is as small as possible. It will be further assumed that $|\dot{\zeta}(t)| \leq N,\ N > 0$, which means that the original disturbance term $\varphi(t)$ must be twice differentiable. In the 2-SM, $s = \xi_2 = 0$, which is exactly equivalent to the condition $s = \dot{s} = 0$, and the *equivalent control* is $w_{eq}(t) = \zeta(t)$. It is assumed that an approximation $\hat{w}_{eq}(t)$ is available (for instance by low pass filtering of the high frequency switching tem (29)) for use in the adaption schemes.

### *B.2 An adaptive super-twisting observer with known N*

Define

$$\delta(t) = k(t) - \frac{1}{\varepsilon_1}\left|w_{eq}(t)\right| - \varepsilon_0 \tag{30}$$

where $0 < \varepsilon_1 < 1$ and $\varepsilon_0 > 0$ is a small real number.

Define the *first layer* of the *dual-layer* adaptation algorithm, associated with the gain $k(t)$ in (29) as

$$\dot{k}(t) = -\left(\rho_0 + \rho(t)\right) sign\left(\delta(t)\right), \quad \rho_0 > 0 \tag{31}$$

The adaptive gain $\rho(t)$ associated with the *second layer* of the adaptation algorithm is chosen to satisfy

$$\dot{\rho}(t) = \gamma\left|\delta(t)\right| + \rho_0\sqrt{\gamma}\, sign\left(e(t)\right), \quad \gamma > 0 \tag{32}$$

where

$$e(t) = \frac{N}{\varepsilon_1} - \rho(t) \tag{33}$$

**Theorem 3.** Consider the system in (18) with a twice differentiable disturbance $\varphi(t)$ subject to $\left|\dot{\varphi}(t)\right| \le H,\ \left|\ddot{\varphi}(t)\right| \le N$, where $N$ is known. Then the sliding mode observer in equations (22), (23), (28) and (29), with the dual layer gain-adaptation in equations (30)-(33) reconstructs the disturbance $h(t)$ in finite time as

$$\hat{h}(t) = -\eta_1\left|s\right|^{1/2} sign(s) - \int k(t)\, sign(s)\, dt \tag{34}$$

Furthermore the variables $\delta(t)$ and $e(t)$ converge to zero in finite time and the gains $k(t)$ and $\rho(t)$ remain bounded.

**Proof.** The $\delta(t)$- and $e(t)$- dynamics are derived as

$$\begin{aligned} \dot{\delta}(t) &= \dot{k}(t) - \frac{1}{\varepsilon_1}\frac{d}{dt}\left|w_{eq}(t)\right| = -\left(\rho_0 + \rho(t)\right) sign\left(\delta(t)\right) - \frac{1}{\varepsilon_1}\frac{d}{dt}\left|\zeta(t)\right| \\ \dot{e}(t) &= -\gamma\left|\delta(t)\right| - \rho_0\sqrt{\gamma}\, sign\left(e(t)\right) \end{aligned} \tag{35}$$

The Lyapunov function candidate

$$V = \frac{1}{2}\delta^2 + \frac{1}{2\gamma}e^2 \tag{36}$$

is considered for dynamics in (35). Its derivative is computed taking into account eq. (33):

$$\begin{aligned} &\dot{V} = \delta\dot{\delta} + \frac{1}{\gamma}e\dot{e} \le -\left(\rho_0 + \rho(t)\right)\left|\delta(t)\right| + \frac{N}{\varepsilon_1}\left|\delta(t)\right| - e\left|\delta(t)\right| - \rho_0\frac{1}{\sqrt{\gamma}}\left|e\right| \le \\ &-\rho_0\left|\delta(t)\right| + \left(\frac{N}{\varepsilon_1} - \rho(t)\right)\left|\delta(t)\right| - e\left|\delta(t)\right| - \rho_0\frac{1}{\sqrt{\gamma}}\left|e\right| = \\ &-\rho_0\left|\delta(t)\right| + e\left|\delta(t)\right| - e\left|\delta(t)\right| - \rho_0\frac{1}{\sqrt{\gamma}}\left|e\right| = \\ &-\rho_0\left|\delta(t)\right| - \rho_0\frac{1}{\sqrt{\gamma}}\left|e\right| = -\rho_0\sqrt{2}\left(\frac{\left|\delta(t)\right|}{\sqrt{2}} + \frac{1}{\sqrt{2\gamma}}\left|e\right|\right) \le -\rho_0\sqrt{2}V^{1/2} \end{aligned} \tag{37}$$

Inequality (37) implies *finite time* convergence $V \to 0$, which means the finite time convergence of $\delta,\ e \to 0$. Therefore, both $\delta$ and $e$ remain bounded. Furthermore, since $k(t) = \delta(t) + \frac{1}{\varepsilon_1}\left|w_{eq}(t)\right| + \varepsilon_0$ and $\rho(t) = \frac{N}{\varepsilon_1} - e(t)$, the variables $k(t), \rho(t)$ also remain bounded. Since $\delta$

= $e$ = 0 in finite time, and from the definition of $\delta(t)$ in (30), the following equality holds (in finite time)

$$k(t) = \left|w_{eq}(t)\right| + \frac{1-\varepsilon_1}{\varepsilon_1}\left|w_{eq}(t)\right| + \varepsilon_0 = \frac{\left|w_{eq}(t)\right|}{\varepsilon_1} + \varepsilon_0 > H \tag{38}$$

This means that equation (26) holds, and therefore selecting $\eta_1$ sufficiently large, guarantees the finite time convergence to zero of the dynamics in (28), (29), and, therefore, $\hat{h}(t)$ in (34) perfectly reconstructs $\hat{h}(t)$ in finite time. Consequently the theorem is proven.

***Remark 3.*** It is easy to show that when the value $N$ exists but is unknown the first layer of the gain adaptation law remains the same as in eq. (31), but the second layer of the adaptation law (32) is simplified to be

$$\dot{\rho}(t) = \gamma\left|\delta(t)\right| \tag{39}$$

### C. Adaptive Continuous HOSM

Again, consider the sliding variable dynamics in (18). In Theorem 2 a continuous HOSM control driven by the super-twisting-based disturbance observer, which drives $s, \dot{s} \to 0$ in the presence of the smooth bounded disturbance $h(t)$, was identified in eqs. (21)-(23). Theorem 3 gives formulations of adaptive super-twisting equivalent control-based disturbance observers that reconstruct the disturbance $h(t)$ in (18). The main result is formulated in the following theorem.

**Theorem 4:** Consider the system (18) with a twice differentiable disturbance $\varphi(t)$ satisfying $\left|\dot{\varphi}(t)\right| \le H$, $\left|\ddot{\varphi}(t)\right| \le N$ and assume $H$ is unknown and $N$ is known. Let the coefficients $\gamma_1, \gamma_2, ..., \gamma_r$ be such that the polynomial $p^r + \gamma_r p^{r-1} + ... + \gamma_2 p + \gamma_1$ is Hurwitz. Then there exists a $\varepsilon \in (0,1)$ such that for every $\alpha \in (1-\varepsilon, 1)$ the origin $\sigma = \dot{\sigma} = ... = \sigma^{(r)} = 0$ is a finite time stable equilibrium under the feedback control in (13), where $\alpha_1, \alpha_2, ..., \alpha_r$ satisfy (20) with $\alpha_{r+1} = 1$ and $\alpha_r = \alpha$; $\varpi$ is defined in (25), (28), (29) and the adaptive scheme is given by equations (30)-(33).
**Proof** straighgforwardly follows Theorems 2 and 3.

### D. Tutorial example

In this section the relative degree 3 system in (18) is simulated. The coefficients of the underlying Hurwitz polynomial $p^3 + \gamma_3 p^2 + \gamma_2 p + \gamma_1$ associated with the controller are selected as $\gamma_1$ = 8, $\gamma_2$ = 12, $\gamma_3$ = 6. The exponents $\alpha_1, \alpha_2, \alpha_3$ in equation (3) are calculated based on the seed $\alpha$ = 0.8. Explicitly they are given by $\alpha_1$ = 0.56, $\alpha_2$ = 0.66 and $\alpha_3$ = 0.8. In the simulations the initial conditions are selected as $\sigma(0) = 1, \dot{\sigma}(0) = 0.5, \ddot{\sigma}(0) = 0$. The disturbance in (18) is taken as $\varphi(t) = 2\sin t$. The parameter $\eta_1$ in the injection term (23) is supposed to be sufficiently large and is taken as $\eta_1 = 4.75$. The other parameters are selected as $\rho_0$ = 1, $\gamma$ = 10 and $\varepsilon_1 = 0.99$, $\varepsilon_0 = 0.01$ = 0.99.

Firstly, the control law in (19), (20) is tested for controlling the unperturbed and perturbed system (18). The results of the simulations are shown in Figs. 3 and 4. In Fig. 3, finite time

convergence to the origin is achieved after 4.5 secs. Fig. 4 shows that neither finite time nor asymptotic stability of the origin is achieved in the presence of the disturbance. Therefore, the finite convergent time controller (19), (20) is not applicable for controlling the perturbed system.

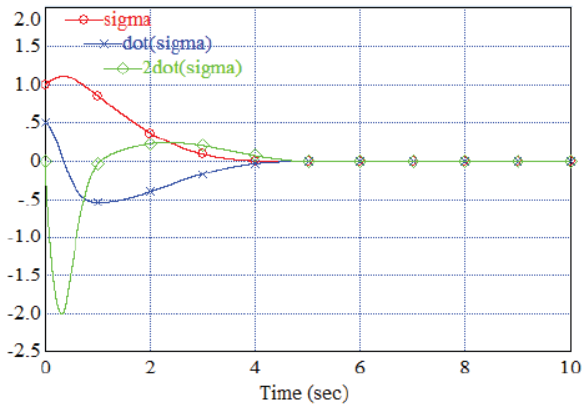


Fig. 3. Finite-time stabilization in unperturbed system (18) by the control in (19), (20)

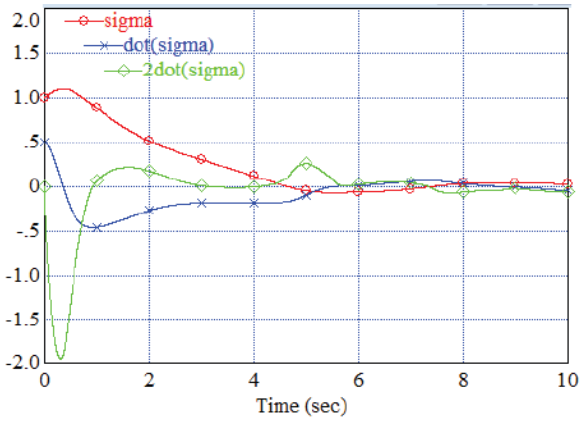


Fig. 4. Finite-time stabilization in perturbed system (18) by the control in (19), (20)

**D1. The case with known** $N$

In this subsection the perturbed system in (18) is simulated using the AHOSM control function defined in (28), (29), (30)-(33). In this case the upper bound $N$ on the disturbance's second derivative is assumed to be known. Since during the simulation the disturbance in eq. (18) is taken as $\varphi(t) = 2\sin t$, the absolute value of its second derivative $\ddot{\varphi}(t) = -2\sin t$ is bounded $|\ddot{\varphi}(t)| \le N = 2$.

It is shown in Fig. 5 that the nominal disturbance-free performance is recovered, and finite time convergence is achieved. Fig. 6 demonstrates the high frequency switching component $w(t)$ and also the adaptive term $\rho(t)$ which is shown to converge to the upper-bound on the 2nd derivative of the disturbance term. It is shown in Fig. 7 that the modulation term $k(t)$ tracks $|\dot{\varphi}(t)|$ very accurately. Fig. 8 shows the control signal $u(t)$, which is clearly smooth and chatter-free, and yet compensates for the disturbance $\varphi(t)$. It is shown in Fig. 9 that $\hat{\varphi}(t)$ accurately reconstructs the unknown disturbance $\varphi(t)$.

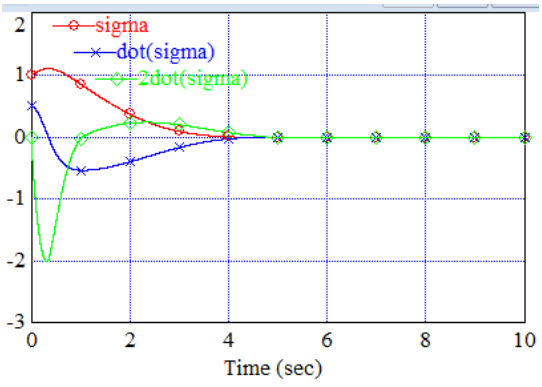


Fig. 5. Finite-time output stabilization of

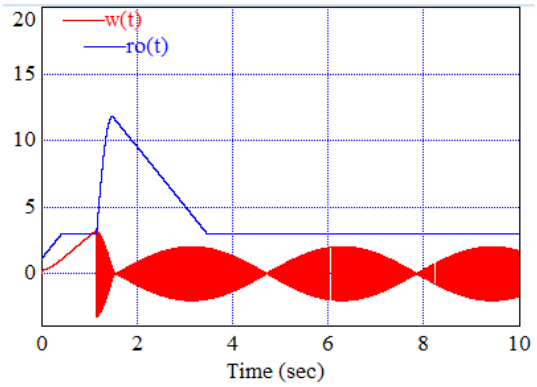


Fig. 6. The second layer of adaptation: $\rho(t)$

perturbed system via adaptive HOSM control with known $N$

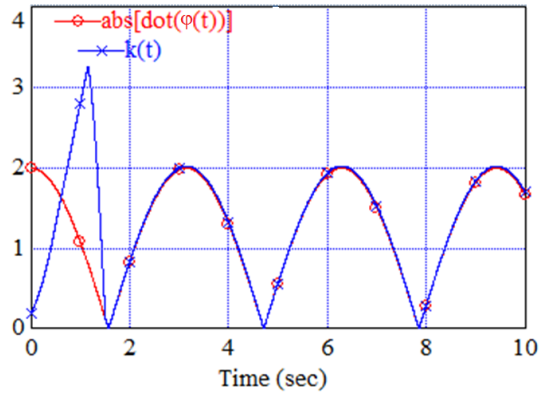


Fig. 7. The first layer of adaptation: $k(t)$ and $|\dot{\varphi}(t)|$ with known $N$

and $\varpi(t)$ with known $N$

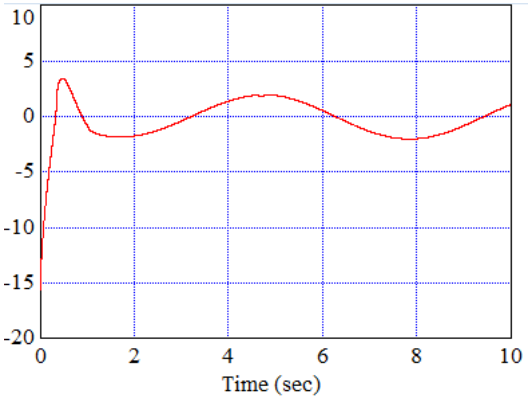


Fig. 8. The continuous adaptive HOSM control function with known $N$

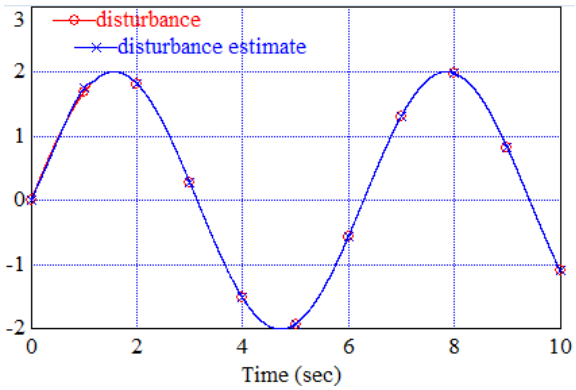


Fig. 9 The disturbance estimation/reconstruction with known $N$

## D2. The case with unknown $N$

In this subsection the perturbed system (18) is simulated while controlled by $u(t)$ in equations (28), (29), (30), (31), (39). In this case the bound $N$ on the second derivative of the disturbance is assumed to be unknown and is not used in the control fuction. It is shown in Fig. 10 that, as in subsection D1, the nominal disturbance-free closed-loop performance is recovered, and finite time convergence is achieved. Figure 11 shows the high frequency switching component $w(t)$ and also the adaptive term $\rho(t)$. It can be seen that $\rho(t)$ remains bounded and asymptotically converges to a value close to 7.0 (which is greater than in the case with known $N=2$). This is consistent with the theoretical study, since the dual-layer adaptive scheme in (28), (29), (30), (31), (39) cannot guarantee that $\rho(t)\to N$. However Fig. 12 shows the modulation term $k(t)$ still tracks $\dot{\varphi}(t)$ very accurately (since in this case $\varepsilon_1 = 0.99 \approx 1$). Finally Fig. 13 shows that $\hat{\varphi}(t)$ accurately tracks the unknown disturbance $\varphi(t)$.

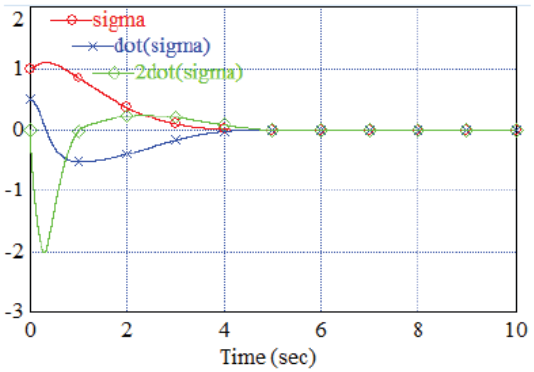


Fig. 10. Finite-time output stabilization of the perturbed system with gain adaptation ( $N$ is unknown)

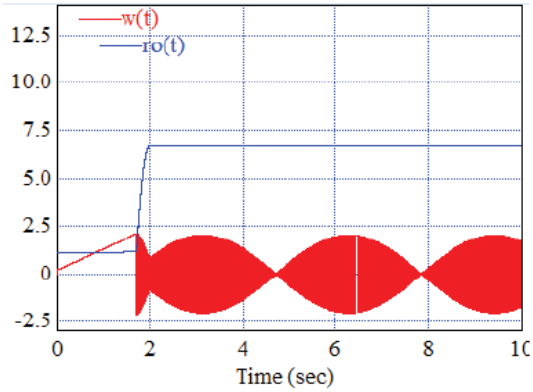


Fig.11 The second layer of adaptation: $\rho(t)$ and $w(t)$ ( $N$ is unknown)

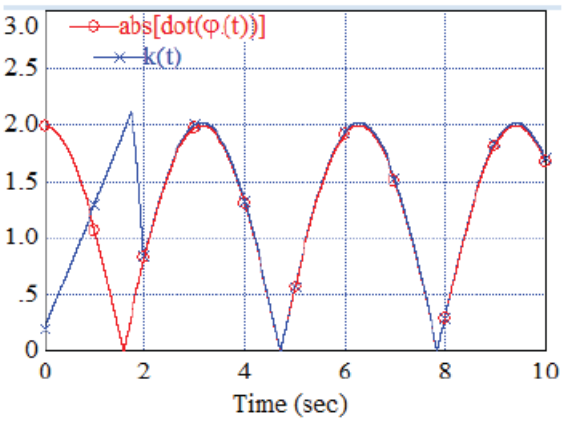


Fig. 12. The first layer of adaptation: $k(t)$ and $|\dot{\varphi}(t)|$ ( $N$ is unknown)

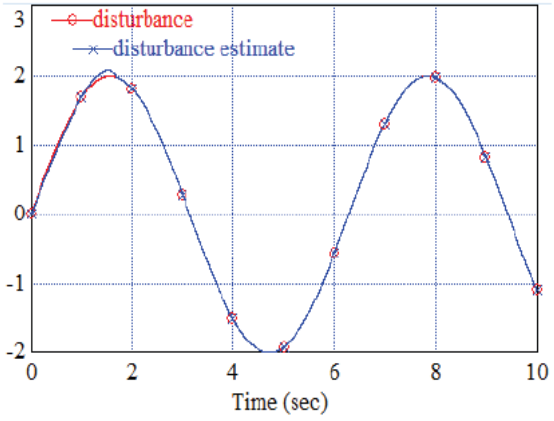


Fig. 13. The disturbance estimation ( $N$ is unknown)

## IV. Design of the Continuous Adaptive Finite Time Convergent Control driven by the Disturbance Observer for Air-Breathing Hypersonic Missile

Here continuous finite time convergent control functions are defined for system (15) in terms of $\omega_1, \omega_2$ for $r = 3$ as

$$\omega_i = \gamma_{3i} \left| e_i^{(2)} \right|^{\alpha_{3i}} sign\left( e_i^{(2)} \right) + \gamma_{2i} |\dot{e}_i|^{\alpha_{2i}} sign(\dot{e}_i) + \gamma_{1i} |e_i|^{\alpha_{1i}} sign(e_i) + \varpi_i \tag{40}$$

where

- $i = \theta, h$,
- the coefficients $\gamma_{1i}$, $\gamma_{2i}$, $\gamma_{3i} > 0$ are selected so that the polynomials $s^3 + \gamma_{3i} s^2 + \gamma_{2i} s + \gamma_{1i}$ are Hurwitz,
- the coefficients $\alpha_{1i}, \alpha_{2i}, \alpha_{3i}$ are defined

$$\alpha_1 = \frac{\bar{\alpha}}{2(2-\bar{\alpha})-1},\ \alpha_2 = \frac{\bar{\alpha}}{2-\bar{\alpha}},\ \alpha_3 = \bar{\alpha} \tag{41}$$

  with $\bar{\alpha} \in (0,1)$.
- The terms $\varpi_i$ are defined in accordance with eqs. (21), (22), (22), (28)-(33)

$$\varpi_i = \eta_{1i}\,|s_i|^{1/2}\,sign(s_i) + \xi_i$$
$$\dot{\xi}_i = k_i(t)sign(s_i), \tag{42}$$
$$s_i = \ddot{e}_i + z_i, \quad \dot{z}_i = -\omega_i - \varpi_i$$

where

$$\delta_i(t) = k_i(t) - \frac{1}{\varepsilon_1}\left|w_{eq_i}(t)\right| - \varepsilon_0$$
$$\dot{k}_i(t) = -\left(\rho_{0i} + \rho_i(t)\right)sign\left(\delta_i(t)\right), \quad \rho_0 > 0 \tag{43}$$
$$\dot{\rho}_i(t) = \gamma\left|\delta_i(t)\right|, \quad \gamma > 0$$

Then, the control laws (3) can be computed as

$$u = \begin{bmatrix}\phi\\ \delta_e\end{bmatrix} = \begin{bmatrix}\int v_1 dt\\ \int v_2 dt\end{bmatrix}; \quad \begin{bmatrix}v_1\\ v_2\end{bmatrix} = G_0^{-1}\begin{bmatrix}\omega_1\\ \omega_2\end{bmatrix} \tag{44}$$

The first and second derivatives of the output tracking errors $e_\theta, e_h$ that are used to compute $\varpi_i$ in (42) are exactly estimated using the HOSM differentiator [7,15] for $k = 4$ as:

The HOSM differentiator is used to obtain the $\ddot{e}_i, \dot{e}_i$. Using the order of HOSM differentiator equal to 4 sufficiently satisfies the differentiation requirements and accuracy of the differentiations. The $\lambda$ values are taken as [15] $\lambda_0 = 1.1, \lambda_1 = 1.5, \lambda_3 = 3, \lambda_4 = 8$

$$\dot{z}_{0i} = -\lambda_4 L_i^{1/5}\left|z_{0i} - e_i\right|^{4/5} sign(z_{0i} - e_i) + z_{1i}$$
$$\dot{z}_{1i} = -\lambda_3 L_i^{1/4}\left|z_{1i} - \dot{z}_{0i}\right|^{3/4} sign(z_{1i} - \dot{z}_{0i}) + z_{2i}$$
$$\dot{z}_{2i} = -\lambda_2 L_i^{1/3}\left|z_{2i} - \dot{z}_{1i}\right|^{3/4} sign(z_{2i} - \dot{z}_{1i}) + z_{3i} \tag{45}$$
$$\dot{z}_{3i} = -\lambda_1 L_i^{1/2}\left|z_{3i} - \dot{z}_{2i}\right|^{3/4} sign(z_{3i} - \dot{z}_{2i}) + z_{4i}$$
$$\dot{z}_{4i} = -\lambda_0 L_i sign(z_{4i} - \dot{z}_{3i})$$

with $i = h, \theta$, $\left|e_i^{(3)}\right| \le L_i$, and $\lambda_0 = 1.1,\ \lambda_1 = 1.5,\ \lambda_2 = 2$ .

The differentiator (45) converges in finite time to

$$z_{0i} = e_i,\ z_{1i} = \dot{e}_i,\ z_{2i} = \ddot{e}_i. \tag{46}$$

## V. Simulation study

### A. Mathematical model of linearized HSM

The nonlinear equations of HSM dynamics (1) were linearized [3,17] at a forward speed $V = 5{,}808\ ft/s$ and an altitude $h = 60{,}000\ ft$:

$$\dot{x} = Ax + Bu + f(t),\ y = Cx \tag{47}$$

where $x = \left[V, \alpha, q, h, \theta\right]^T$, the external disturbance $f(t)$ is a smooth function, norm-bounded together with its first and second derivatives: $\|f(t)\| \le F_0,\ \left\|\dot{f}(t)\right\| \le F_1,\ \left\|\ddot{f}(t)\right\| \le F_2,\ F_0, F_1, F_2 > 0$, the matrix $B = B_0 + \Delta B(t) + B_n(t)$ with $B_0$ a known matrix, while $\Delta B(t)$ is a norm-bounded constant perturbation matrix, $B_n(t)$ is a perturbation matrix with periodical entries (both multiplicative perturbation matrices are unmatched), and the controllable matrices $A, B_0$ are given as in [3]:

$$A=\begin{bmatrix} -0.0063291 & -16.996 & 0 & 5.6665\times10^{-5} & -31.986 \\ -2.0235\times10^{-6} & -0.44804 & 1 & 4.843\times10^{-7} & 0 \\ -0.00022922 & 27.667 & 0 & -9.8466\times10^{-8} & 0 \\ 2.2663\times10^{-18} & -5807.5 & 0 & 0 & 5807.5 \\ 0 & 0 & 1 & 0 & 0 \end{bmatrix} \tag{48}$$

$$B_0=\begin{bmatrix} -127.24 & -0.06884 & -25.618 & 0 & 0 \\ 98.641 & -0.0058935 & -0.40286 & 0 & 0 \end{bmatrix}^T \tag{49}$$

The output matrix is defined

$$C=\begin{bmatrix} 0 & 0 & 0 & 1 & 0 \\ 0 & 0 & 0 & 0 & 1 \end{bmatrix} \tag{50}$$

The constant disturbance multiplicative matrix is presented as a percentage of the nominal entries of the matrix $B_0$ and has the following form

$$\Delta B(t)=\begin{bmatrix} 5.563\% & 85.475\% & 7.806\% & 0 & 0 \\ 18.788\% & -18.776\% & 99.752\% & 0 & 0 \end{bmatrix}^T \tag{51}$$

Its entries can be non-constant, but bounded.

The matrix $B_n(t)$ has the form

$$B_n(t)=2.6\cdot10^{-3}\sin(12t)\cdot\begin{bmatrix} 1 & 1 & 1 & 1 & 1 \\ 1 & 1 & 1 & 1 & 1 \end{bmatrix}^T \tag{52}$$

It is worth noting that $CB=\mathbf{0},\ \mathbf{0}\in\mathbb{R}^{2\times2}$.

The unmatched additive time-varying vector-disturbance $f(t)$ is taken as

$$f(t)=\left[0.8+0.6\mu(t),\ 2\cdot10^{-4}+10^{-3}\mu(t),\ 0.02+0.5\mu(t),\ 2\cdot10^{-4}+0.01\mu(t),\ 2\cdot10^{-4}+10^{-4}\mu(t)\right]^T \tag{53}$$

where $\mu(t)=\sin(t)+1.4\sin(2t)$.

The Hurwitz constant in the HOSM differentiator (29) is taken as $L=9.2\cdot10^5$. The parameters of the adaptation law in (43) are selected as $\rho_{0h}=1.1,\ \rho_{0\theta}=2,\ \varepsilon_o=15,\ \varepsilon_1=0.99,\ \gamma_h=120,\ \gamma_\theta=250$.

### B. Validation of the adaptive continuous HOSM controller

The simulation results of the HSM in the terminal phase (47)-(53) using the adaptive continuous finite convergent higher order sliding mode controller driven by the continuous higher order disturbance observer (40)-(45) with the second layer adaptive gain taken in the simplified form of (39), i.e. $\dot{\rho}_i(t)=\gamma|\delta_i(t)|$, with the unmatched time-varying external disturbances $f(t)$ in (53) and the multiplicative perturbations $\Delta B(t)$ and $B_n(t)$ in (51) and (52) respectively are presented in Figs. 14-21.

High accuracy attitude tracking is demonstrated in Figs. 14-16. Maximum target penetration is provided, which can be seen in Figs. 14-16 and 21, where the altitude, pitch, and downrange distance errors are near zero. It should be noted that the downrange distance accuracy is within 1.67 ft of the desired target location. The control inputs time history in Fig. 17 shows continuous control functions. The fuel air ratio control does saturate at zero for short time in order to stay within the fuel/air ratio limits of [0, 1.5]. Figure 18 demonstrates how the adaptive observer injection term gains adjust while compensating the perturbations.

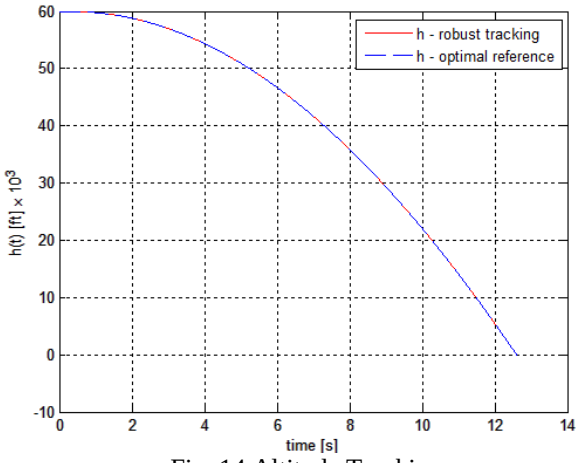


Fig. 14 Altitude Tracking

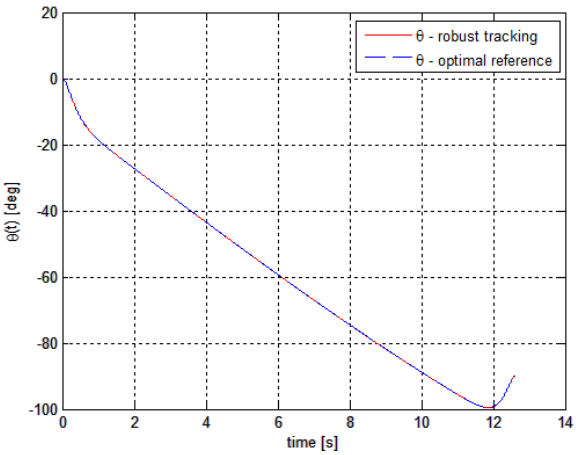


Fig. 15 Pitch Angle Tracking

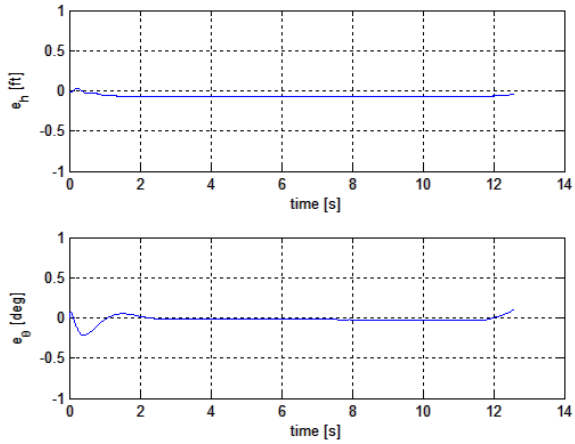


Fig. 16 Altitude and Pitch Angle Errors

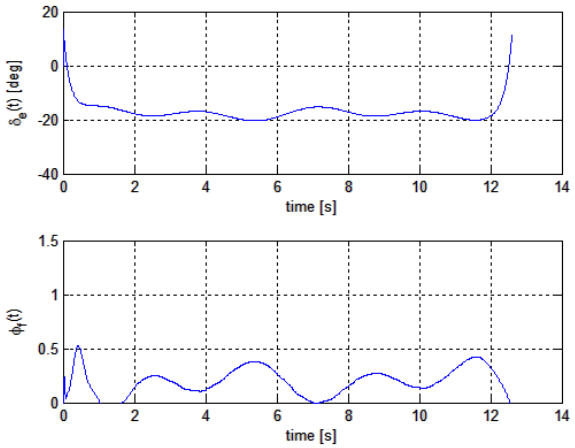


Fig. 17: Control Inputs

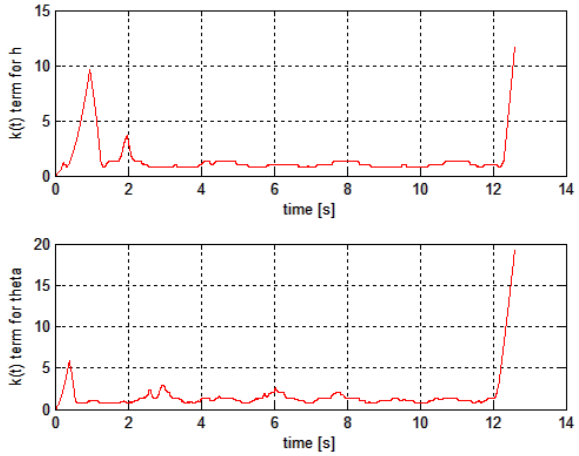


Fig. 18 Adaptive first layer control gains

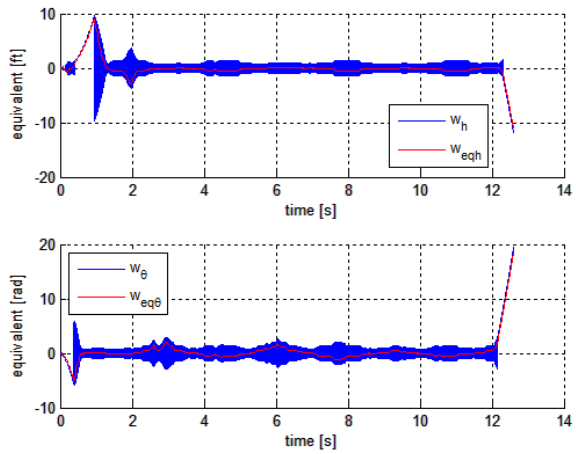


Fig. 19 Adaptive control terms that are hidden behind integrals

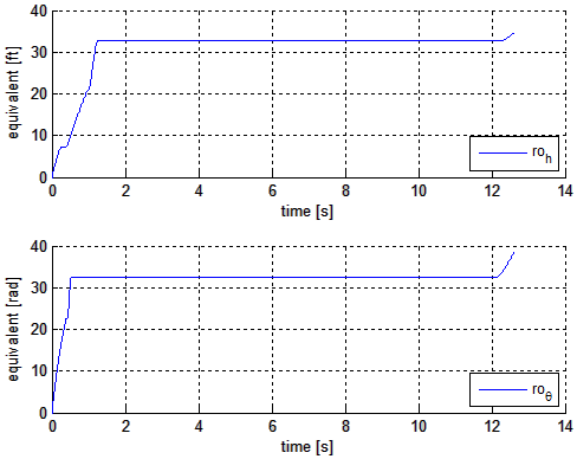


Fig. 20 Adaptive second layer control gains

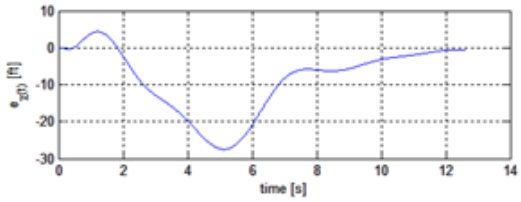


Fig. 21 Downrange tracking error

Figure 19 shows the adaptive control high frequency switching terms that are hidden behind the integrals. Their amplitudes adjust just to compensate for the additive and multiplicative disturbances and are in line with the adaptive gains $k_h(t)$ and $k_\theta(t)$. The time history of the second layer adaptive gains $\rho_h(t)$ and $\rho_\theta(t)$ that support the adaptation of the first layer gains $k_h(t)$ and $k_\theta(t)$ are shown in Fig. 20. It can be seen that the first and second layer adaptive gains are bounded. Therefore, the application of the proposed control algorithms to HSM control is feasible and achieves excellent results in the presence of bounded additive and multiplicative disturbances, whose nature and format are unknown.

## VI. Conclusion

In this paper control of a hypersonic missile (HSM) in the terminal phase is considered. Two control inputs, elevator deflection and the throttling of the air-breathing engine are used to control the HSM. The output variables to control are defined as the pitch angle and the HSM altitude. The adaptive double-layer continuous higher order sliding mode controller driven by the higher order continuous sliding mode observer that is robust to the perturbations is proposed and rigorously studied. In order to improve the smoothness of the control laws, the controller was designed in terms of the derivatives of the control functions. Curve-fitted approximations of the aerodynamic forces and moments are not needed in the proposed control design approach. A linearized model of a HSM was used for testing the proposed control algorithms. The proposed controller has been studied in a challenging end-game scenario with matched and unmatched additive and multiplicative periodic disturbances. The output tracking errors $e_\theta, e_h$ are accurately driven to zero by the continuous adaptive HOSM controller in the presence of matched and unmatched perturbations. The proposed adaptive control technique demonstrates the capability to accurately control the hypersonic missile in the terminal phase target, while maximizing the target penetration.

## References


[1] Bolender, M. A. and Doman, D. B., "Nonlinear Longitudinal Dynamical Model of an Air-Breathing Hypersonic Vehicle," *Journal of Spacecraft and Rockets*, Vol. 44, No. 2, Apr. 2007, pp. 374–387.

[2] Parker J., Serrani A., Yurkovich S., Bolender M., Doman D. Control-oriented modeling of an air-breathing hypersonic vehicle, *Journal of Guidance, Control, and Dynamics*, Vol. 30, No.3, 2007, pp. 856–869.

[3] Mehta S. S., MacKunis W., Subramanian S., Pasiliao C. L. Nonlinear Control of Hypersonic Missiles for Maximum Target Penetration. *AIAA Guidance, Navigation, and Control Conference*, 2012.

[4] Fiorentini L., Serrani A., Bolender MA., and Doman, DB. Nonlinear Robust Adaptive Control for Flexible Air-breathing Hypersonic Vehicles. *Journal of Guidance, Control, and Dynamics*, Vol. 32, No. 2, 2009, pp. 402–417.

[5] Sigthorsson D., Jankovsky P., Serrani A., Yurkovich S., Bolender M., and Doman, D. Robust Linear Output Control of an Air breathing Hypersonic Vehicle. *Journal of Guidance, Control, and Dynamics*, Vol. 31, No. 4, 2008, pp. 1052–1066.

[6] Serrani A., Zinnecker AM., Fiorentini L., Bolender MA., and Doman DB. Integrated adaptive guidance and control of constrained nonlinear air-breathing hypersonic vehicle models. *American Control Conferenc*e, June 2009, pp. 3172–3177.

[7] Levant A. Higher-order sliding modes, differentiation and output feedback control. *International Journal of Control*, **76**(9/10), 2003, pp. 924-941.

[8] Bhat S.P., and Bernstein DS. Geometric homogeneity with applications to finite time stability. *Math. Control Signals Systems*, Vol. 17, 2005, pp. 101–127.

[9] Levant A. Quasi-continuous high-order sliding-mode controllers. *IEEE Trans. Automat. Control*, Vol**.** 50, No**.** 11, 2006, pp. 1812-1816.

[10] Levant A. (Levantovsky LV.). Sliding order and sliding accuracy in sliding mode control. *International Journal of Control*, Vol. 86, 1993, pp. 1247-1263.

[11] Fiorentini L., Serrani A., Bolender MA., and Doman DB. Robust Nonlinear Sequential Loop Closure Control Design for an Air-breathing Hypersonic Vehicle Model. *Proceedings of American Control Conference*, 2008, pp. 3458-3463.

[12] Shtessel Y. and Tournes C. Integrated Higher Order Sliding Mode Guidance and Autopilot for Dual Control Missiles. *AIAA Journal on Guidance, Control, and Dynamics*, Vol. 32, No. 1, 2009, pp. 79-94.

[13] Tournes V., Shtessel Y., and Shkolnikov I. Autopilot for Missiles Steered by Aerodynamic Lift and Divert Thrusters Using Nonlinear Dynamic Sliding Manifolds. *AIAA Journal on Guidance, Control, and Dynamics*, Vol. 29, No. 3, 2006, pp. 617-625.

[14] Xiaoxiang Hua, LigangWua, Changhua Hub, and Huijun Gao. Adaptive sliding mode tracking control for a flexible air-breathing hypersonic vehicle. *Journal of the Franklin Institute*, Vol. 349, 2012, pp. 559–577.

[15] Shtessel Y, Edwards C., Fridman L., and Levant A. *Sliding Mode Control and Observation*, Birkhauser, Springer, New York, 2014.

[16] Utkin VI. and Poznyak AS. Adaptive sliding mode control with application to super-twisting algorithm: Equivalent control method. *Automatica*, 49:39–47, 2013.

[17] Yu Polk. Hypersonic Missile Control In Terminal Mode Using Continuous Higher Order Sliding Mode Control Driven by Disturbance Observer. ProQuest LLC, 2013.